I&EC research
Industrial & Engineering Chemistry Research

pubs.acs.org/IECR
Article

Core–Shell Catalyst Pellets for Reaction Heat Release Control in Fixed-Bed Reactors

Ronny Tobias Zimmermann* and Kai Sundmacher*

Cite This: *Ind. Eng. Chem. Res.* 2024, 63, 7556–7564
Read Online

ABSTRACT: Core–shell catalyst pellets are an opportunity for fixed-bed reactor operation, where heat management is a challenge. Core–shell catalyst pellets consist of a catalytically active core surrounded by an inert, porous shell. The shell enables controllable heat release rates at high temperatures by limiting mass transport to the active material in the pellet core and, thus, effectively prevents thermal runaways. In addition, the inert shell influences the selectivity of the reaction system. This paper investigates the applicability of core–shell catalyst pellets in a general chemical system involving one or two equilibrium reactions, by deriving catalyst effectiveness factors, the selectivity, and a mean apparent activation energy for predicting parametrically sensitive conditions with the "practical design criterion". Experimental results are presented, which confirm the mathematical predictions and demonstrate the effectiveness of core–shell pellets for CO_2 methanation. The results highlight the role of the catalyst pellet design in ensuring safe and efficient reactor operation. The results are readily applicable to other chemical processes and provide valuable insights into the opportunities of catalyst pellet design for efficient reactor operation.

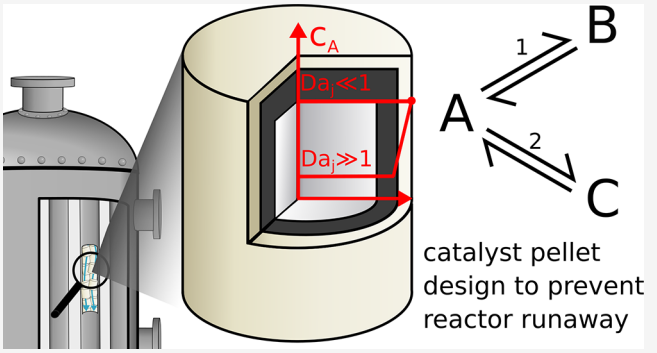

INTRODUCTION

Chemical process routes for renewable fuel synthesis are currently investigated due to the opportunity of storing electrical energy in chemical compounds. In these processes, excess renewable energy is used to produce hydrogen via electrochemical water splitting. This so-called green hydrogen is then converted to e-fuels or ammonia. In particular, the synthesis of e-fuels also offers the opportunity to reduce carbon dioxide emissions by using them as a reactant. However, the intermittent supply of excess renewable energy makes these processes technologically challenging, due to unsteady process conditions, or expensive, due to the need for large intermediate buffer units.[1−3]

Wall-cooled multitubular fixed-bed reactors, consisting of parallel tubes surrounded by a coolant, have emerged as the key technology for e-fuel and ammonia synthesis. These reactors offer simple construction, scalability, and a high space-time yield. As the reactor is often the central unit of a production plant, it plays a crucial role in determining the overall economics of the process. Therefore, reactor design has been the subject of continuous research for decades, using both experimental and model-based approaches, and has gained new interest in the light of flexible reactor operation. In particular, the design of fixed-bed reactors for carrying out highly exothermic, heterogeneously catalyzed gas-phase reactions requires a thorough understanding of the underlying physicochemical processes, as these reactors are often prone to thermal instability, which is a challenge, especially during load-flexible operation.[4−6]

Heat management is, therefore, the central aspect of fixed-bed reactor design, and considerable effort is devoted to predicting the temperature profile in catalytic fixed-beds, as it is critical for economic and safety reasons, but at the same time quite complex. In the simplest case, the reactant consumption in the reactor is neglected, and the temperature profile can be derived by solving the steady-state energy balance equation in the axial direction of the fixed-bed:

$$u\rho c_p \frac{dT}{dz} = q_{rel} - q_{rem} \tag{1}$$

The heat release rate q_{rel} and removal rate q_{rem} may be expressed for a single reaction as

$$q_{rel} = -\Delta_r H \zeta \eta(T) \sigma_{int}(T) \tag{2}$$

Received: January 2, 2024
Revised: March 28, 2024
Accepted: April 1, 2024
Published: April 22, 2024

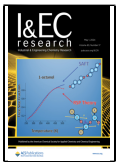

https://doi.org/10.1021/acs.iecr.3c04587
Ind. Eng. Chem. Res. 2024, 63, 7556–7564

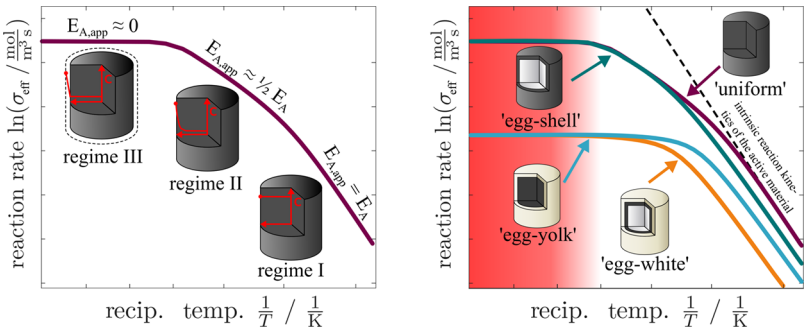

Figure 1. Arrhenius diagrams—Left: Apparent activation energies and schematic reactant concentration profiles in different catalyst pellet operating regimes. Right: Comparison of the effective reaction rates of different catalyst pellet designs. Catalyst deactivation temperatures are indicated by the red background.

$$q_{\mathrm{rem}} = \frac{4U}{D}(T - T_{\mathrm{cool}}) \tag{3}$$

where ζ is the catalyst pellet dilution factor and η is the catalyst effectiveness factor. The intrinsic reaction rate σ_{int} typically follows an Arrhenius-type temperature dependence with the activation energy E_A:

$$\frac{\mathrm{d}\ln\sigma_{\mathrm{int}}}{\mathrm{d}T^{-1}} = -\frac{E_A}{R} \tag{4}$$

As shown by Semenov,[7] such systems exhibit a subcritical state with finite temperature rise and a supercritical state with unlimited temperature rise, known as thermal runaway. The reason for thermal runaways is rooted in the nonlinear Arrhenius dependence of the heat release rate on temperature, whereas the heat removal rate depends linearly on the difference between the fixed-bed temperature and the coolant temperature. The transition point between the two states depends on the reactor design and the operating parameters.

In real systems, either all reactants are consumed or chemical equilibrium is reached, so the temperature rise always remains finite and a maximum temperature is observed at the so-called hot-spot. Downstream of the hot-spot, the temperature approaches that of the coolant. However, sensitivity toward reactor parameters may still occur and a small change can lead to large changes in the hot-spot temperature. Consequently, sensitive reactor conditions have to be avoided or handled very carefully, which is especially true during load-flexible reactor operation, as the hot-spot temperature increase is often related to a decrease in selectivity, catalyst deactivation, or even material damage.[8,9] Much research has been conducted to predict such sensitive conditions.[10−15] A simple but insightful approach is to estimate the conditions for safe reactor operation by ensuring that the heat removal rate increases faster than the heat release rate with the temperature at the reactor hot-spot position z_{hs}, known as the "slope condition".

$$\left.\frac{\mathrm{d}q_{\mathrm{rel}}}{\mathrm{d}T}\right|_{z=z_{\mathrm{hs}}} < \left.\frac{\mathrm{d}q_{\mathrm{rem}}}{\mathrm{d}T}\right|_{z=z_{\mathrm{hs}}} \tag{5}$$

In the context of this work, the "slope condition" can be expressed more conveniently by dividing both sides by the heat release rate and multiplying both sides with $-T^2$. By equating the right-hand side of eq 1 with zero, it is evident that the heat release rate is equal to the heat removal rate at the hot-spot,

$$u\rho c_p \left.\frac{\mathrm{d}T}{\mathrm{d}z}\right|_{z=z_{\mathrm{hs}}} = 0 \leftrightarrow \left.q_{\mathrm{rel}}\right|_{z=z_{\mathrm{hs}}} = \left.q_{\mathrm{rel}}\right|_{z=z_{\mathrm{hs}}} \tag{6}$$

and thus the slope conditions can be rewritten as

$$-\left.\frac{T^2}{q_{\mathrm{rel}}}\frac{\mathrm{d}q_{\mathrm{rel}}}{\mathrm{d}T}\right|_{z=z_{\mathrm{hs}}} > -\left.\frac{T^2}{q_{\mathrm{rem}}}\frac{\mathrm{d}q_{\mathrm{rem}}}{\mathrm{d}T}\right|_{z=z_{\mathrm{hs}}} \tag{7}$$

$$\rightarrow \left.\frac{\mathrm{d}\ln q_{\mathrm{rel}}}{\mathrm{d}T^{-1}}\right|_{z=z_{\mathrm{hs}}} > \left.\frac{\mathrm{d}\ln q_{\mathrm{rem}}}{\mathrm{d}T^{-1}}\right|_{z=z_{\mathrm{hs}}} \tag{8}$$

By inserting eqs 2 and 3 into this modified "slope condition", a simple design criterion is obtained for predicting parametrically sensitive reactor conditions, which is known as "practical design criterion":[12,15]

$$E_{\mathrm{A,app}} = E_A + R\frac{\mathrm{d}\ln(\eta)}{\mathrm{d}T^{-1}} < \frac{RT_{\mathrm{hs}}^2}{T_{\mathrm{hs}} - T_{\mathrm{cool}}} \tag{9}$$

If the inequality is satisfied, then there are no parametrically sensitive conditions according to the criterion. It is obvious that the term on the right-hand side is always greater than zero, as exothermic reactions by their nature produce hot-spot temperatures that exceed the coolant temperature. Consequently, the inequality remains satisfied if the left-hand side of the criterion, which by definition is the apparent activation energy of the chemical reaction, is zero, indicating a heat release rate independent of temperature.

In its current form, the "practical design criterion" also incorporates the influence of catalyst pellet design, as captured by the catalyst effectiveness factor. This factor describes the influence of transport processes within the catalyst pellets on the effective reaction rate. For isothermal pellets with uniform, "egg-shell", "egg-white", and "egg-yolk" distribution of the active material, the following approximate equation holds for arbitrary reaction kinetics:[16]

$$\eta = \frac{\sigma_{\mathrm{eff}}}{\sigma_{\mathrm{int}}} = \frac{1}{(1+\delta)^{n+1}}\left[\frac{\Phi}{\tanh(\Gamma\Phi)} + \frac{\Phi^2}{\mathrm{Bi}}\right]^{-1} \tag{10}$$

https://doi.org/10.1021/acs.iecr.3c04587
Ind. Eng. Chem. Res. 2024, 63, 7556−7564

$$\approx \begin{cases} \dfrac{\Gamma}{(1+\delta)^{(n+1)}} & \text{Regime I: } \Phi \ll 1 \\ \dfrac{1}{\Phi(1+\delta)^{(n+1)}} & \text{Regime II: } \Phi \gg 1 \vee \mathrm{Bi} \to \infty \\ \dfrac{\mathrm{Bi}}{\Phi^2(1+\delta)^{(n+1)}} & \text{Regime III: } \Phi \gg 1 \end{cases} \tag{11}$$

$$\text{with } \Gamma = 1 - \frac{V_{ic}}{V_{am}} \text{ and } \delta = \frac{R_{is}}{R_{am}} \tag{12}$$

In this equation, n is the catalyst pellet shape factor, δ is the dimensionless inert shell radius, Γ is the fraction of active material in the pellet core, Bi is the generalized Biot number, and Φ is the generalized Thiele modulus. By choosing an appropriate Thiele modulus, this equation asymptotically describes the kinetic regime (Regime I), as well as the regimes of internal mass transport limitation (Regime II), and external mass transfer limitation by the gas boundary layer or mass transport limitation by the inert shell (Regime III), which are shown in Figure 1. As the intrinsic reaction rate often exhibits the most pronounced temperature dependence, all other temperature dependencies can be approximately neglected. This allows to derive simple correlations of the apparent activation energies in the three regimes:

$$E_{A,app} = E_A - R\frac{\mathrm{d}\ln(\eta)}{\mathrm{d}\ln(\Phi)}\frac{\mathrm{d}\ln(\Phi)}{\mathrm{d}T^{-1}} \tag{13}$$

$$\approx \begin{cases} E_A & \text{Regime I: } \eta \propto \Phi^0 \\ \frac{1}{2}E_A & \text{Regime II: } \eta \propto \Phi^{-1} \\ 0 & \text{Regime III: } \eta \propto \Phi^{-2} \end{cases} \tag{14}$$

$$\text{with } E_{A,app} = -R\frac{\mathrm{d}\ln(\sigma_{eff})}{\mathrm{d}T^{-1}} \tag{15}$$

$$\text{and } \Phi \propto \sqrt{\sigma_{int}} \tag{16}$$

In Regime III, the reaction rate is so fast that mass transfer or transport to the catalytically active material becomes the rate-determining step. As this process is assumed to be temperature-independent in this derivation, the apparent activation energy is zero. Consequently, the "practical design criterion" is indeed always satisfied in this case, independent of the other reactor or catalyst pellet parameters, and parametrically sensitive conditions are avoided. A more detailed study of this limiting scenario yields $E_{A,app} = m\,RT$ (where m is approximately 1.5 for molecular diffusion and $m = 0.5$ for Knudsen diffusion[17]), which remains significantly smaller than the activation energy observed of most heterogeneously catalyzed reactions.

If the primary resistance of mass transfer occurs in the gas boundary layer surrounding the pellets, then this effect is highly dependent on reactor operating conditions and becomes prominent only at very high reactor temperatures, where catalyst deactivation might be an issue. However, it is possible to shift Regime III to temperatures where catalyst deactivation does not occur.[18−20] This can be achieved by applying an inert shell onto the catalyst pellets, as the mass transport resistance of the shell is in series with the mass transfer resistance of the gas boundary layer, as shown in Figure 1.

Taking the example of the CO_2 methanation system given in Figure 2, it has been demonstrated that this approach offers

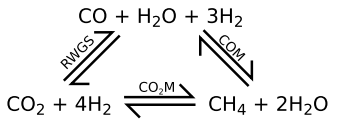

Figure 2. Carbon dioxide methanation (CO_2M) with reverse water gas shift reaction (RWGS) as side reaction and carbon monoxide methanation (COM) as a linear combination thereof. Adapted from Zimmermann et al.[21] published under Creative Commons License CC-BY 4.0. Copyright 2022, Elsevier.

significant advantages over conventional fixed-bed dilution of uniform catalyst pellets with inert pellets.[16] This is because fixed-bed dilution is temperature-independent, resulting in a substantial reduction in the reaction rate not only at high temperatures but also at low temperatures, which are present toward the reactor outlet. However, this is where no dilution of the catalyst pellets is required, leading to low space-time yields. Using multiple sections of differing fixed-bed dilution to compensate for this results in complex reactor behavior, with multiple hot-spots. Furthermore, fixed-bed pellet dilution does not alter the apparent activation energy, as the "practical design criterion" does not depend on the catalyst pellet dilution ratio. Thus, while fixed-bed dilution may decrease the hot-spot temperature, parametric sensitivity might still occur.

The feasibility of preparing core−shell catalyst pellets by fluidized-bed coating of commercially available spherical Ni/Al_2O_3 pellets has been demonstrated and the conducted catalytic activity experiments confirm the computationally predicted results.[21] Furthermore, it is shown that the effective methanation rate of the pellets exhibits vanishing apparent activation energy at elevated temperatures. It is also observed that the coated pellets exhibited a significantly higher methane selectivity. This increase in selectivity is attributed to the interaction between the mass transport processes occurring in the inert shell and the chemical equilibrium within the center of the catalyst pellets when mass transport to the catalytically active material is the rate-determining step.

The aim of this study is to investigate these relationships, namely, the avoidance of thermal runaway and the shift in selectivity, in more general situations using manageable mathematical expressions. The focus is on a reaction system consisting of two parallel equilibrium reactions, which are frequently encountered, e.g., when CO_2 is used as a reactant. For this purpose, the effective reaction rates of the system are computed first, taking into account the influence of the mass transport resistance of the inert shell. The selectivity and apparent activation energy of the system are then derived as a function of the resulting parameters. The conclusions drawn from these analyses are then discussed qualitatively on experimental results obtained for cylindrical Ru/Al_2O_3 "egg-white" catalyst pellets used in CO_2 methanation.

EFFECTIVE REACTION RATES OF SIMULTANEOUS EQUILIBRIUM REACTIONS

The effect of an inert shell on the effective reaction rates of the catalyst pellets is captured by the catalyst effectiveness factors. As reviewed in the book of Aris,[17] deriving the catalyst effectiveness factors for real reaction systems can be mathematically sophisticated and often requires numerical solution approaches, even for systems involving only a single reaction. The complexity increases when multiple reactions with arbitrary kinetics are involved as these reactions influence each other in

https://doi.org/10.1021/acs.iecr.3c04587
Ind. Eng. Chem. Res. 2024, 63, 7556−7564

various ways. For example, successive reactions may resemble parallel reactions, as demonstrated by Wei[22,23] by solving a system of first-order reactions.

However, it is possible to derive simplified equations, which are asymptotically accurate for the limiting cases of very high and very low reaction rates, as shown above for a single reaction. In the following sections, such equations are derived for a system with two linearly independent equilibrium reactions in an "egg-white" pellet as shown in Figure 3. The respective equations for

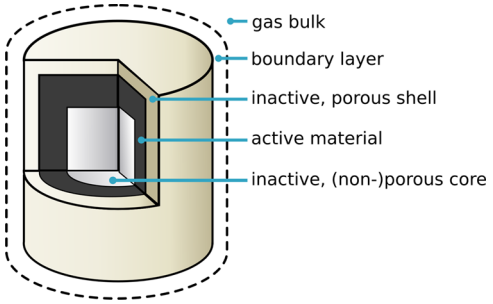

Figure 3. Schematic representation of the modeled catalyst pellets.

"egg-yolk", "egg-shell", and uniform catalyst pellets are obtained by simplification of the result. It is furthermore not relevant whether the equilibrium reactions are parallel or consecutive as both cases can be converted into each other. The derivation of the catalyst effectiveness factors starts from the Gaussian integral theorem:

$$\int_{A_{is}} N_i \, \mathrm{d}A = \int_{V_{am}} \sum_{j=1}^{2} (\nu_{i,j}\sigma_j) \, \mathrm{d}V \tag{17}$$

which states that the flow of each component N_i across the external surface of the pellet A_{is} is equal to its consumption (or production) in the pellet volume at steady-state conditions. The integrals can be simplified by assuming a constant flux, independent of angle, over the entire external surface of the catalyst pellet and no gradients within the catalytically active material in the inert core:

$$N_i|_{r=R_{is}} A_{is} = V_{am} \sum_{j=1}^{2} (\nu_{i,j}\sigma_j) \tag{18}$$

As shown in Figure 1, this assumption holds for Regimes I and III. Cases where gradients within the active material appear are mathematically more sophisticated and are beyond the scope of this work. As $N_i|_{r=R_{is}} A_{is} = N_i|_{r=R_{am}} A_{am}$, this equation can be rewritten

$$N_i|_{r=R_{am}} = \frac{V_{am}}{A_{am}} \sum_{j=1}^{2} (\nu_{i,j}\sigma_j) = \frac{\Gamma R_{am}}{n+1} \sum_{j=1}^{2} (\nu_{i,j}\sigma_j) \tag{19}$$

with $n = 0$ for sealed slabs, $n = 1$ for sealed cylinders and $n = 2$ for spheres. Dealing with gradients within the inert shell is straightforward as long as the individual component fluxes do not interact with each other. Assuming the mass flow through the inert shell follows Fick's first law of diffusion, Morbidelli and Varma[24] have shown that the mass transfer resistance of the inert shell and the boundary layer add up as series resistance:

$$N_i|_{r=R_{am}} = \frac{c_{i,bulk} - c_{i,am}}{\frac{R_{am}^n}{\beta_i R_{is}^n} + \frac{R_{am}^n \Delta}{D_{i,is}}} \tag{20}$$

$$\text{with} \quad \Delta = \begin{cases} R_{is} - R_{am} & \text{for} \quad n = 0 \\ \ln(R_{is}/R_{am}) & \text{for} \quad n = 1 \\ R_{am}^{-1} - R_{is}^{-1} & \text{for} \quad n = 2 \end{cases} \tag{21}$$

As further steps toward the catalyst effectiveness factors are the stoichiometric relations, which describe the relationship between the i concentrations to j artificial potentials, called reaction extents ξ_j. They are based on the mass conservation of chemical reactions and their application as well as their limitations have been discussed by several authors.[25−27] The relations read

$$N_i = -\sum_{j}^{\mathfrak{n}_{reac}} \nu_{i,j} \frac{\mathrm{d}\xi_j}{\mathrm{d}r} \tag{22}$$

Inserting Fick's first law of diffusion

$$N_i = -D_{i,am} \frac{\mathrm{d}c_i}{\mathrm{d}r} \tag{23}$$

and integrating toward the gas bulk gives

$$D_{i,am}(c_{i,bulk} - c_{i,am}) = -\sum_{j}^{\mathfrak{n}_{reac}} \nu_{i,j}\xi_{j,am} \tag{24}$$

with $\xi_{j,bulk} = 0$ by definition. In this step, it was implicitly assumed that $D_{i,am}/D_{i,is}$ and $D_{i,am}/\beta_i$ are the same for each component. The necessity of this assumption is elaborated in detail by Gavalas.[27] Substituting eqs 20 and 24 into eq 19, multiplying both sides by the inverse stoichiometric matrix, and non-dimensionalizing the equation yields

$$\psi_j = \frac{\Phi_j^2}{\mathrm{Bi}} f_j(\psi_1, \psi_2) = \mathrm{Da}_j f_j(\psi_1, \psi_2) \tag{25}$$

$$\text{with} \quad \psi_j = \frac{\xi_j}{\xi_{j,eq}}, \quad f_j = \frac{\sigma_j}{\sigma_{j,int}}, \quad \Phi_j = \frac{\Gamma R_{am}}{n+1} \sqrt{\frac{\sigma_{j,int}}{-\xi_{j,am}}} \tag{26}$$

$$\mathrm{Bi} = \frac{n+1}{\left(\frac{R_{am}^{n-1} D_{i,am}}{\beta_i R_{is}^n} + \Delta \frac{R_{am}^{n-1} D_{i,am}}{D_{i,is}} \right)} \tag{27}$$

where Da_j is a Damköhler number of the second kind, which relates the reaction rate in the absence of transport phenomena at bulk conditions to the maximum mass transport rates at equilibrium conditions in the active material. The respective equilibrium reaction extent $\xi_{j,eq}$ is obtained by solving the equilibrium conditions

$$K_j = \prod_{i}^{\mathfrak{n}_{comp}} p_i^{\nu_{i,j}} \tag{28}$$

together with stoichiometric relations eq 24. If the dimensionless reaction rate $f_j(\psi_1, \psi_2)$ are simple expressions, this equation system is solvable for the dimensionless reaction extents ψ_j, from which it is possible to calculate the catalyst effectiveness factors. However, in general $f_j(\psi_1, \psi_2)$ can be nonlinear functions, and thus no straightforward solution is possible. It is therefore

https://doi.org/10.1021/acs.iecr.3c04587
Ind. Eng. Chem. Res. 2024, 63, 7556−7564

suitable to express the reaction rates as a Taylor-Polynomial under bulk conditions, which is truncated after the linear term:

$$f_1 = 1 + \frac{\partial f_1}{\partial \psi_1}|_{\psi_1=0,\psi_2=0}\psi_1 + \frac{\partial f_1}{\partial \psi_2}|_{\psi_1=0,\psi_2=0}\psi_2 \tag{29}$$

$$f_2 = 1 + \frac{\partial f_2}{\partial \psi_1}|_{\psi_1=0,\psi_2=0}\psi_1 + \frac{\partial f_2}{\partial \psi_2}|_{\psi_1=0,\psi_2=0}\psi_2 \tag{30}$$

The derivatives can be approximated without computing the gradients by setting the reaction rates equal to zero at the chemical equilibrium. Hereby, a distinction must be made between only one reaction in chemical equilibrium and both reactions in chemical equilibrium. The respective equilibrium reaction extents ($\xi_{2,\xi_1=0,\mathrm{eq}}$, $\xi_{1,\xi_2=0,\mathrm{eq}}$) are obtained by solving the equilibrium conditions eq 28 together with the stoichiometric relations eq 24 as well:

$$\frac{\partial f_1}{\partial \psi_1} \approx -\omega_1 \quad \frac{\partial f_1}{\partial \psi_2} \approx -(1-\omega_1) \tag{31}$$

$$\frac{\partial f_2}{\partial \psi_1} \approx -(1-\omega_2) \quad \frac{\partial f_2}{\partial \psi_2} \approx -\omega_2 \tag{32}$$

$$\text{with} \quad \omega_1 = \frac{\xi_{1,\mathrm{eq}}}{\xi_{1,\xi_2=0,\mathrm{eq}}} \quad \text{and} \quad \omega_2 = \frac{\xi_{2,\mathrm{eq}}}{\xi_{2,\xi_1=0,\mathrm{eq}}} \tag{33}$$

Inserting the linearized reaction rates into eq 27, and solving the equation system for the dimensionless reactions extents yields

$$\psi_1 = \mathrm{Da}_1 \frac{1 + \mathrm{Da}_2(\omega_1+\omega_2-1)}{1 + \omega_1\mathrm{Da}_1 + \omega_2\mathrm{Da}_2 + \mathrm{Da}_1\mathrm{Da}_2(\omega_1+\omega_2-1)} \tag{34}$$

$$\psi_2 = \mathrm{Da}_2 \frac{1 + \mathrm{Da}_1(\omega_1+\omega_2-1)}{1 + \omega_1\mathrm{Da}_1 + \omega_2\mathrm{Da}_2 + \mathrm{Da}_1\mathrm{Da}_2(\omega_1+\omega_2-1)} \tag{35}$$

On this basis, the catalyst effectiveness factor can now be calculated for both reactions:

$$\eta_1 = \frac{\int_0^{(1+\delta)^{n+1}} f_1 \varrho^n \mathrm{d}\varrho}{\int_0^{(1+\delta)^{n+1}} \varrho^n \mathrm{d}\varrho} = \frac{\Gamma}{(1+\delta)^{n+1}} \frac{1 + \mathrm{Da}_2(\omega_1+\omega_2-1)}{1 + \omega_1\mathrm{Da}_1 + \omega_2\mathrm{Da}_2 + \mathrm{Da}_1\mathrm{Da}_2(\omega_1+\omega_2-1)} \tag{36}$$

$$\approx \begin{cases} \dfrac{\Gamma}{(1+\delta)^{n+1}} & \text{for} \quad \mathrm{Da}_1 \ll 1 \vee \mathrm{Da}_2 \ll 1 \\ \dfrac{\Gamma}{(1+\delta)^{n+1}}\mathrm{Da}_1^{-1} & \text{for} \quad \mathrm{Da}_1 \gg 1 \vee \mathrm{Da}_2 \gg 1 \end{cases} \tag{37}$$

By swapping the coefficients ($1 \leftrightarrow 2$), the catalyst effectiveness factor of the second reaction is obtained. The derived catalyst effectiveness factors can now be used to describe the catalyst pellet behavior in different situations. Due to the numerous involved parameters, the focus in the following is on cases, where either both reaction rates are slow ($\mathrm{Da}_j \ll 1$) or fast ($\mathrm{Da}_j \gg 1$) compared to the mass transport to the active material. Of particular interest for a multicomponent multireaction system are the selectivity of the catalyst pellets and the apparent activation energy, which are discussed below.

Influence on the Selectivity. If the reactants exhibit different effective diffusion coefficients, then the mass transport rates through the inert shell also differ. For example, in the limiting case of Knudsen diffusion, the ratio of diffusion coefficients is $D_i/D_\mathrm{k} = \sqrt{M_\mathrm{k}/M_i}$. For this reason, not only the concentrations but also the ratios of the concentrations in the catalyst pellets can differ significantly from those in the gas bulk under the influence of mass transfer or transport resistance, which in turn affects the ratio of the reaction rates. With the catalyst effectiveness factors given above, the differential selectivity of the catalyst pellets is calculated as

$$S_1 = \frac{\eta_1\sigma_{1,\mathrm{int}}}{\eta_1\sigma_{1,\mathrm{int}} + \eta_2\sigma_{2,\mathrm{int}}} \tag{38}$$

$$\approx \begin{cases} \dfrac{\sigma_{1,\mathrm{int}}}{\sigma_{1,\mathrm{int}} + \sigma_{2,\mathrm{int}}} & \text{for} \quad \mathrm{Da}_1 \ll 1 \vee \mathrm{Da}_2 \ll 1 \quad \text{(a)} \\ \dfrac{\xi_{1,\mathrm{eq}}}{\xi_{1,\mathrm{eq}} + \xi_{2,\mathrm{eq}}} & \text{for} \quad \mathrm{Da}_1 \gg 1 \vee \mathrm{Da}_2 \gg 1 \quad \text{(b)} \end{cases} \tag{39}$$

$$S_2 = 1 - S_1 \ \text{(in any case)} \tag{40}$$

As expected, the selectivity of a chemical reaction system is not affected by mass transfer or transport when both reaction rates are comparatively slow, and the inert material in the core and in the shell merely serves as dilution of the active material. However, the situation is more complex when both reactions are fast. The selectivity then corresponds to the ratio of the reaction extents in chemical equilibrium under the influence of mass transport or transfer to the active material. In general, these must be calculated numerically because of the nonlinearity of the equilibrium conditions. However, the instructive special case of linear equilibrium conditions allows for an explicit solution, which is given in the Supporting Information of Zimmermann et al.[21] and is repeated here for convenience:

$$S_1 = \frac{\frac{D_\mathrm{B}(K_1 p_{\mathrm{A,eq}} - p_{\mathrm{B,bulk}})}{D_\mathrm{C}(K_2 p_{\mathrm{A,eq}} - p_{\mathrm{C,bulk}})}}{1 + \frac{D_\mathrm{B}(K_1 p_{\mathrm{A,eq}} - p_{\mathrm{B,bulk}})}{D_\mathrm{C}(K_2 p_{\mathrm{A,eq}} - p_{\mathrm{C,bulk}})}} \tag{41}$$

$$\text{with} \quad \frac{p_{\mathrm{A,eq}}}{p_{\mathrm{A,bulk}}} = \frac{1 + \frac{D_\mathrm{B}}{D_\mathrm{A}}\frac{p_{\mathrm{B,bulk}}}{p_{\mathrm{A,bulk}}} + \frac{D_\mathrm{C}}{D_\mathrm{A}}\frac{p_{\mathrm{C,bulk}}}{p_{\mathrm{A,bulk}}}}{1 + \frac{D_\mathrm{B}}{D_\mathrm{A}}K_1 + \frac{D_\mathrm{C}}{D_\mathrm{A}}K_2} \tag{42}$$

The equation yields the selectivity of the catalyst pellets, exemplarily depicted in Figure 4, if the mass transport to the active material is rate determining. The equation simplifies significantly if no products are present in the gas bulk:

$$S_1 = \frac{\frac{D_\mathrm{B}K_1}{D_\mathrm{C}K_2}}{1 + \frac{D_\mathrm{B}K_1}{D_\mathrm{C}K_2}} \tag{43}$$

Evidently, the selectivity is shifted toward the reaction with the product, which has the higher diffusion coefficient in the inert shell, compared to what is expected from the gas bulk equilibrium. If this is not the target product, it is possible to influence the selectivity by changing the gas bulk composition

https://doi.org/10.1021/acs.iecr.3c04587
Ind. Eng. Chem. Res. 2024, 63, 7556−7564

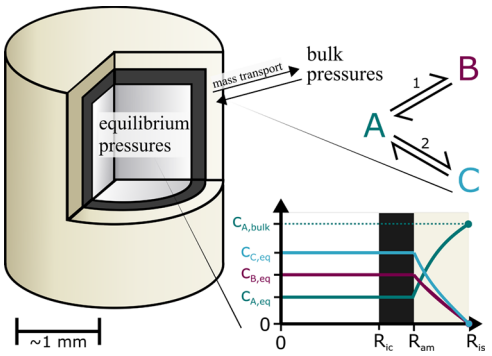

Figure 4. Simple reaction system catalyzed by an "egg-white" pellet, where the mass transport to the active material is the rate-determining step. Adapted from Zimmermann et al.[21] published under Creative Commons License CC-BY 4.0. Copyright 2022, Elsevier.

according to Le Chatelier's principle, e.g., by providing the products of the undesired reaction. Furthermore, it is notable that the selectivity does not depend on the distribution of the active material, but solely on the ratio of the diffusion coefficients.

Mean Apparent Activation Energy. For each of the two reactions, an individual apparent activation energy can be calculated straightforwardly from the definition in eq 15. However, to apply the "practical design criterion" defining an average activation energy is suitable. It is derived by inserting the total heat release rate of both reactions into eq 8:

$$q_{\mathrm{rel}} = \sum_{j=1}^{2} -\Delta_{\mathrm{r}}H_j \eta_j \sigma_{j,\mathrm{int}} \tag{44}$$

$$\rightarrow \overline{E}_{\mathrm{A,app}} = -R \frac{\mathrm{d}\ln\left(\sum_{j=1}^{2} -\Delta_{\mathrm{r}}H_j \eta_j \sigma_{j,\mathrm{int}}\right)}{\mathrm{d}T^{-1}} \tag{45}$$

$$= \frac{\sum_{j=1}^{2} \Delta_{\mathrm{r}}H_j \eta_j \sigma_{j,\mathrm{int}} E_{j,\mathrm{A,app}}}{\sum_{j=1}^{2} \Delta_{\mathrm{r}}H_j \eta_j \sigma_{j,\mathrm{int}}} \tag{46}$$

$$= \begin{cases} \dfrac{\sum_{j=1}^{2} \Delta_{\mathrm{r}}H_j \sigma_{j,\mathrm{int}} E_{j,\mathrm{A}}}{\sum_{j=1}^{2} \Delta_{\mathrm{r}}H_j \sigma_{j,\mathrm{int}}} & \text{for} \quad \mathrm{Da}_1 \ll 1 \vee \mathrm{Da}_2 \ll 1 \\ 0 & \text{for} \quad \mathrm{Da}_1 \gg 1 \vee \mathrm{Da}_2 \gg 1 \end{cases} \tag{47}$$

$$\text{with} \quad E_{j,\mathrm{A,app}} = E_{j,\mathrm{A}} - R \sum_{l}^{2} \frac{\mathrm{d}\ln \eta_j}{\mathrm{d}\ln \mathrm{Da}_l} \frac{\mathrm{d}\ln \mathrm{Da}_l}{\mathrm{d}T^{-1}} \tag{48}$$

For the natural logarithm to be defined, it is implicitly assumed that the total heat release rate is positive. Otherwise, the system is overall endothermic, and no runaway is observed. If both reaction rates are relatively small (Regime I), the apparent activation energy of the reactant consumption rate is the weighted average of the individual reaction rates. Thus, slow reactions, or reactions with small reaction enthalpy, do not contribute as much as reactions with high reaction rates or reactions with high reaction enthalpies. Endothermic reactions even decrease the risk of thermal runaway. Furthermore, it is observed that neither the inert core nor the inert shell influences the apparent activation energy if no transport of transfer limitations are present. In the opposite case, where mass transport or transfer to the active material is rate determining for both reactions (Regime III), the apparent activation energy is zero even in the presence of two equilibrium reactions. Evidently, eq 9 is thus satisfied and no parametrically sensitive conditions and consequentially no thermal runaways are expected even in the presence of multiple reactions.

EXPERIMENTAL RESULTS ON "EGG-WHITE" PELLETS

In the following, the conclusions derived above are discussed on experimental results of Ru/Al_2O_3 "egg-white" catalyst pellets. As seen in eq 37, an inert core does not contribute to the effective reaction rate if mass transport to the active material is rate determining. Thus, "egg-white" pellets exhibit the opportunity of saving potentially costly active material. With CO_2 methanation as example, it has been shown that employing 'egg-white' pellets can save up to 45.2% of the active material mass in a fixed-bed reactor.[28]

Cylindrical 0.5 wt % Ru/Al_2O_3 "egg-shell" catalyst pellets (Sigma-Aldrich) have been coated with an inert shell. If not mentioned otherwise, the preparation and testing is identical to that described by Zimmermann et al.[21] for spherical catalyst pellets. However, since the flat surfaces of the cylinders lead to strong adhesion between the individual pellets, the suspension has been slightly modified. Overall, the mass fractions in the suspension are 5% pseudoboehmite powder, 10% α-alumina powder, 1.35% polyvinyl alcohol, and 83.65% distilled water. Samples taken after 0 min (calcined catalyst pellets without

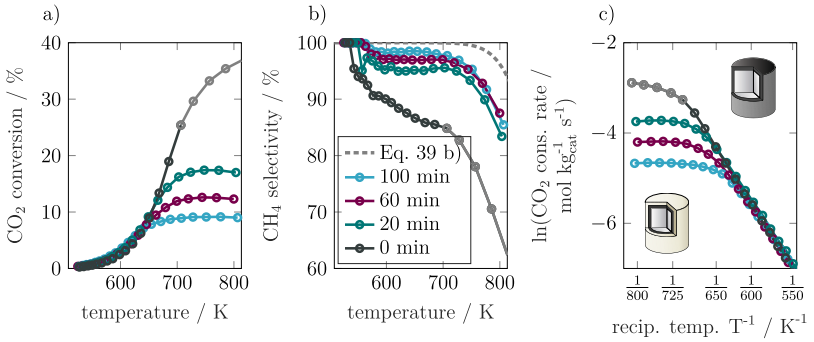

Figure 5. Carbon dioxide conversion (a), methane selectivity (b), and carbon dioxide consumption rate (c) for coated and uncoated Ru/Al_2O_3 cylinders at p = 1.5 bar, x_{CO_2} = 0.1, x_{H_2} = 0.4, and x_{He} = 0.5. Data points with X_{CO_2} > 20% are marked as gray as no differential reaction conditions can be assumed in this case. The sample taken at 0 min has not been introduced into the fluidized-bed but is otherwise treated in the same way as the fluidized-bed coated samples. In addition, the selectivity at the limit of external mass transport limitation of both reactions is given according to eq 39b.

https://doi.org/10.1021/acs.iecr.3c04587
Ind. Eng. Chem. Res. 2024, 63, 7556−7564

coating), 20, 60, and 100 min of process time are examined in detail.

The fluidized-bed coating procedure used results in very low overspray and uniform growth of the pellets from a Sauter diameter of 3.6−4.0 mm after 100 min of coating time, in accordance to the results by Zimmermann et al.[21] Thus, catalytic activity tests have been carried out in a laboratory scale reactor, and the results are shown in Figure 5. Under the specified conditions, detectable conversions of carbon dioxide are observed from about 525 K.

It is evident that the inert shell has a significant influence on the catalytic activity of the catalyst pellets. While the conversion of the uncoated catalyst pellets shows an increasing trend over the investigated temperature range, it reaches an almost constant plateau at about 700 K for the coated samples. Furthermore, the obtained conversion decreases with increasing coating thickness and, as expected from eq 40 as well as previous results,[21] the methane selectivity increases. A comparison between catalyst pellets without an inert shell and those with the thickest shell at 773 K reveals an increase in methane selectivity of approximately 10% at 700 K. Furthermore, the selectivity of the sample taken after 60 min is the same as that of the sample taken after 100 min, indicating the selectivity to be independent of the shell thickness in the limiting case. Compared to the theoretical selectivity, when both reaction rates are at the chemical equilibrium in the catalyst pellet cores, the experimentally observed selectivities follow the expected behavior but are slightly lower. A possible explanation for this is the exothermicity of the methanation reaction, which may result in an increase of the pellet core temperature compared to the bulk temperature, which, in turn, shifts the chemical equilibrium.

The high selectivity toward methane allows a direct correlation between carbon dioxide conversion and methanation reaction rate, facilitating the derivation of the apparent activation energy in the Arrhenius diagram shown in Figure 5c. It is observed that at low temperatures the apparent activation energy is the same for all samples and exhibits a value of about 81 kJ/mol. However, for the coated samples the activation energy starts to decrease and reaches a plateau with increasing temperature. The magnitude of the plateau decreases with increasing coating thickness, indicating that mass transport through the inert shell is the rate-determining step in agreement with the theoretical expectation.

CONCLUSIONS

Understanding and controlling mass transport phenomena at the catalyst pellet scale provides opportunities for improving fixed-bed reactor operation. For example, it is known that core−shell catalyst pellets, consisting of an active core surrounded by an inert porous shell, can effectively prevent runaway conditions in wall-cooled fixed-bed reactors with a single reaction.

This study extends the results to a general reaction system with two simultaneous equilibrium reactions. At first, the effectiveness factors for both reactions are derived based on the Gaussian integral theorem. The effectiveness factors allow for the calculation of the selectivity and a mean apparent activation energy for the reaction system, which can be used in the "practical design criterion". These performance parameters are studied in the limiting cases of simultaneously low and high Damköhler numbers. It is found that an inert shell on the catalyst pellets effectively prevents parametrically sensitive reactor conditions also in the presence of two equilibrium reactions.

The results derived on a mathematical basis are supported by experimental results obtained on cylindrical Ru/Al_2O_3 "egg-white" pellets, validating the expected behavior. Furthermore, both mathematical and experimental investigations show that the inert shell induces a shift in selectivity as the chemical equilibrium is attained in the core of the pellet when mass transport to the active material is the rate-determining step. However, due to the nonlinearities inherent to the equilibrium conditions, numerical solution methods are generally required to determine the preferred reaction. As a general guideline, it is expected that the reaction associated with the product exhibiting faster diffusion through the inert shell is favored, compared to what is expected from the selectivity of the gas bulk equilibrium. The mathematical and experimental approaches presented in this study can be extended straightforwardly to other processes to investigate the design of safe and cost-effective reactors with core−shell catalyst pellets.

AUTHOR INFORMATION

Corresponding Authors

Ronny Tobias Zimmermann − *Chair for Process Systems Engineering, Otto von Guericke University, Magdeburg 39106, Germany;* orcid.org/0000-0002-6598-0180; Phone: +49 (0)391 6110-360; Email: ronny.zimmermann@mpi-magdeburg.mpg.de; Fax: +49 (0)391 6110-353

Kai Sundmacher − *Chair for Process Systems Engineering, Otto von Guericke University, Magdeburg 39106, Germany; Department of Process Systems Engineering, Max Planck Institute Magdeburg, Magdeburg 39106, Germany;* orcid.org/0000-0003-3251-0593; Phone: +49 (0)391 6110-360; Email: sundmacher@mpi-magdeburg.mpg.de; Fax: +49 (0)391 6110-353

Complete contact information is available at: https://pubs.acs.org/10.1021/acs.iecr.3c04587

Notes

The authors declare no competing financial interest.

ACKNOWLEDGMENTS

The authors thank Prof. Dr.-Ing. Jens Bremer for the discussion on the parametric sensitivity of wall-cooled fixed-bed reactors. Furthermore, the authors thank Prof. Dr.-Ing. Lothar Mörl and Dr.-Ing. Vesselin Idakiev for coating the pellets and for the in-depth discussion regarding the operation of fluidized-bed coating. This research work was also supported by the Center of Dynamic Systems 364 (CDS), which is funded by the EU program EFRE (European Regional Development Fund). Ronny Tobias Zimmermann is also affiliated to the International Max Planck Research School (IMPRS) for Advanced Methods in Process and Systems Engineering in Magdeburg.

NOMENCLATURE

Latin

A, external surface area/m^2
c, concentration/mol m^{-3}
c_p, heat capacity/J mol^{-1} K^{-1}
d, tube diameter/m
D, effective diffusion coefficient/m^2 s^{-1}
E, energy/J mol^{-1}
f, dimensionless reaction rate/−
$\Delta_r H$, reaction enthalpy/J mol^{-1}
K, equilibrium constant/−

https://doi.org/10.1021/acs.iecr.3c04587
Ind. Eng. Chem. Res. 2024, 63, 7556−7564

M, molar mass/kg mol^{-1}
n, pellet shape factor/−
$\mathbb{n}$, number of···/−
N, flux/mol m^{-2} s^{-1}
p, pressure/Pa
q, heat release rate/mol m^{-3} s^{-1}
r, pellet radius/m
R, ideal gas constant/J mol^{-1} K^{-1}
S, selectivity/−
T, temperature/K
u, gas velocity/m s^{-1}
V, total volume enclosed by area A/m^3
x, mole fraction/−
X, conversion/−
z, axial fixed-bed coordinate/m

Greek

β, mass transfer coeffcient/−
Γ, dimensionless active material volume fraction/−
δ, dimensionless shell thickness/−
ζ, catalyst pellet dilution factor/−
ρ, density/−
ϱ, dimensionless pellet radius/−
η, catalyst effectivness factor/−
ν, stoichiometric coefficient/−
ξ, reaction extent/mol m^{-1} s^{-1}
σ, reaction rate/mol m^{-3} s^{-1}
Φ, Thiele modulus/−
ψ, dimensionless reaction extent/−
ω, dimensionless equilibrium reaction extent/−

Dimensionless numbers

Bi, Generalized Biot Number/−
Da, Damköhler Number of the second kind/−

Indices

i,*k*, component index
j,*l*, reaction index
A, activation
am, active material
app, apparent
bulk, gas bulk
cool, coolant
comp, component
eff, effective
eq, equilibrium
hs, hot-spot
ic, inert core
int, intrinsic
is, inert shell
reac, reaction
rel, release
rem, removal

REFERENCES

(1) Wulf, C.; Zapp, P.; Schreiber, A. Review of Power-to-X Demonstration Projects in Europe. *Front. Energy Res.* **2020**, *8*, 191.
(2) Gahleitner, G. Hydrogen from renewable electricity: An international review of power-to-gas pilot plants for stationary applications. *Int. J. Hydrogen Energy* **2013**, *38*, 2039−2061.
(3) Götz, M.; Lefebvre, J.; Mörs, F.; McDaniel Koch, A.; Graf, F.; Bajohr, S.; Reimert, R.; Kolb, T. Renewable Power-to-Gas: A technological and economic review. *Renewable Energy* **2016**, *85*, 1371−1390.
(4) Fache, A.; Marias, F.; Guerré, V.; Palmade, S. Optimization of fixed-bed methanation reactors: Safe and efficient operation under transient and steady-state conditions. *Chem. Eng. Sci.* **2018**, *192*, 1124−1137.
(5) Kreitz, B.; Wehinger, G. D.; Turek, T. Dynamic simulation of the CO_2methanation in a micro-structured fixed-bed reactor. *Chem. Eng. Sci.* **2019**, *195*, 541−552.
(6) Bremer, J.; Sundmacher, K. Operation range extension via hot-spot control for catalytic CO_2 methanation reactors. *Reaction Chemistry & Engineering* **2019**, *4*, 1019−1037.
(7) Semenov, N. N. Theories of combustion process. *Z. Phys. Chem.* **1928**, *48*, 571−582.
(8) Stoessel, F. *Thermal Safety of Chemical Processes*; John Wiley & Sons, Ltd.: Weinheim, 2020.
(9) Kao, C.-S.; Hu, K.-H. Acrylic reactor runaway and explosion accident analysis. *Journal of Loss Prevention in the Process Industries* **2002**, *15*, 213−222.
(10) Bilous, O.; Amundson, N. R. Chemical reactor stability and sensitivity: II. Effect of parameters on sensitivity of empty tubular reactors. *AIChE J.* **1956**, *2*, 117−126.
(11) Morbidelli, M.; Varma, A. A generalized criterion for parametric sensitivity: Application to thermal explosion theory. *Chem. Eng. Sci.* **1988**, *43*, 91−102.
(12) Bashir, S.; Chovan, T.; Masri, B. J.; Mukherjee, A.; Pant, A.; Sen, S.; Vijayaraghavan, P.; Berty, J. M. Thermal runaway limit of tubular reactors, defined at the inflection point of the temperature profile. *Ind. Eng. Chem. Res.* **1992**, *31*, 2164−2171.
(13) Kummer, A.; Varga, T. Completion of thermal runaway criteria: Two new criteria to define runaway limits. *Chem. Eng. Sci.* **2019**, *196*, 277−290.
(14) Bremer, J.; Sundmacher, K. Novel Uniqueness and Multiplicity Criteria for Non-Isothermal Fixed-Bed Reactors, Exemplied for Catalytic CO_2 Methanation. *Front. Energy Res.* **2020**, *8*, No. 549298.
(15) Kummer, A.; Varga, T. What do we know already about reactor runaway? − A review. *Process Safety and Environmental Protection* **2021**, *147*, 460−476.
(16) Zimmermann, R. T.; Bremer, J.; Sundmacher, K. Multi-Period Design Optimization of Flexible Fixed-Bed Reactors by Stoichiometry-Based Model Reduction. *Comput.-Aided Chem. Eng.* **2021**, *50*, 947−952.
(17) Aris, R. The mathematical theory of diffusion and reaction in permeable catalysts: The theory of the steady state. In *The Mathematical Theory of Diffusion and Reaction in Permeable Catalysts*; Clarendon Press, 1975.
(18) Zimmermann, R. T.; Bremer, J.; Sundmacher, K. Optimal catalyst particle design for flexible fixed-bed CO_2 methanation reactors. *Chemical Engineering Journal* **2020**, *387*, No. 123704.
(19) Baratti, R.; Gavriilidis, A.; Morbidelli, M.; Varma, A. Optimization of a nonisothermal nonadiabatic fixed-bed reactor using dirac-type silver catalysts for ethylene epoxidation. *Chem. Eng. Sci.* **1994**, *49*, 1925−1936.
(20) Mazidi, S. K.; Sadeghi, M. T.; Marvast, M. A. Optimization of Fischer−Tropsch process in a fixed-bed reactor using non-uniform catalysts. *Chem. Eng. Technol.* **2013**, *36*, 62−72.
(21) Zimmermann, R. T.; Weber, S.; Bremer, J.; Idakiev, V.; Pashminehazar, R.; Sheppard, T. L.; Mörl, L.; Sundmacher, K. Core-shell catalyst pellets for effective reaction heat management. *Chemical Engineering Journal* **2023**, *457*, No. 140921.
(22) Wei, J. Intraparticle diffusion effects in complex systems of first order reactions I. The effects in single particles. *J. Catal.* **1962**, *1*, 526−537.
(23) Wei, J. Intraparticle diffusion effects in complex systems of first order reactions II. The influence of diffusion on the performance of chemical reactors. *J. Catal.* **1962**, *1*, 538−546.
(24) Morbidelli, M.; Varma, A. On shape normalization for non-uniformly active catalyst pellets—II. *Chem. Eng. Sci.* **1983**, *38*, 297−305.
(25) Burghardt, A. Transport phenomena and chemical reactions in porous catalysts for multicomponent and multireaction systems. *Chemical Engineering and Processing: Process Intensification* **1986**, *20*, 229−244.

https://doi.org/10.1021/acs.iecr.3c04587
Ind. Eng. Chem. Res. 2024, 63, 7556−7564

(26) Jackson, R. *Transport in porous catalysts*; Elsevier Scientific Publishing Comp.: Amsterdam, 1977.
(27) Gavalas, G. R. *Nonlinear differential equations of chemically reacting systems*; Springer: Berlin, Heidelberg, 1968.
(28) Zimmermann, R. T.; Bremer, J.; Sundmacher, K. Optimal Catalyst-Reactor Design for Load-Flexible CO2 Methanation by Multi-Period Design Optimization. *Comput.-Aided Chem. Eng.* **2022**, *49*, 841−846.

https://doi.org/10.1021/acs.iecr.3c04587
Ind. Eng. Chem. Res. 2024, 63, 7556−7564